Stem Cell Reports

Article

Inactivation of STAT3 Signaling Impairs Hair Cell Differentiation in the Developing Mouse Cochlea

Qianqian Chen,[1,2] Yizhou Quan,[1,2] Naitao Wang,[1] Chengying Xie,[2] Zhongzhong Ji,[1,2] Hao He,[2,3] Renjie Chai,[4] Huawei Li,[5] Shankai Yin,[3] Y. Eugene Chin,[6] Xunbin Wei,[1,2,]* and Wei-Qiang Gao[1,2,3,]*

[1]State Key Laboratory of Oncogenes and Related Genes, Renji-MedX Stem Cell Research Center, Ren Ji Hospital, School of Biomedical Engineering, Shanghai Jiao Tong University, Shanghai 200030, China
[2]Med-X Research Institute & School of Biomedical Engineering, Shanghai Jiao Tong University, Shanghai 200030, China
[3]The Affiliated Six People's Hospital, Med-X Research Institute and School of Biomedical Engineering, Shanghai Jiao Tong University, Shanghai 200030, China
[4]MOE Key Laboratory of Developmental Genes and Human Disease, Institute of Life Sciences, Southeast University, Nanjing 210096, China
[5]Otorhinolaryngology Department of Affiliated Eye and ENT Hospital, State Key Laboratory of Medical Neurobiology, Fudan University, Shanghai 200031, China
[6]China Key Laboratory of Stem Cell Biology, Institute of Health Sciences, Shanghai Institutes for Biological Sciences, Chinese Academy of Sciences-Shanghai Jiao Tong University School of Medicine, Shanghai 200031, China
*Correspondence: xwei01@sjtu.edu.cn (X.W.), gao.weiqiang@sjtu.edu.cn (W.-Q.G.)
http://dx.doi.org/10.1016/j.stemcr.2017.05.031

SUMMARY

Although STAT3 signaling is demonstrated to regulate sensory cell differentiation and regeneration in the zebrafish, its exact role is still unclear in mammalian cochleae. Here, we report that STAT3 and its activated form are specifically expressed in hair cells during mouse cochlear development. Importantly, conditional cochlear deletion of *Stat3* leads to an inhibition on hair cell differentiation in mice *in vivo* and *in vitro*. By cell fate analysis, inactivation of STAT3 signaling shifts the cell division modes from asymmetric to symmetric divisions from supporting cells. Moreover, inhibition of Notch signaling stimulates STAT3 phosphorylation, and inactivation of STAT3 signaling attenuates production of supernumerary hair cells induced by a Notch pathway inhibitor. Our findings highlight an important role of the STAT3 signaling during mouse cochlear hair cell differentiation and may have clinical implications for the recovery of hair cell loss-induced hearing impairment.

INTRODUCTION

Hearing loss, often caused by irreversible damage to hair cells, has been affecting millions of people in the world. Hair cells, located adjacent to surrounding supporting cells, are mechanosensory cells that can directly convert sound into electrical signals (Fujioka et al., 2015). Hair cell differentiation emerges at the mid-basal region of sensory epithelium at embryonic day 14 (E14), and subsequently extends along the entire epithelium in basal-to-apical and medial-to-lateral fashions (Kelley, 2006). Previous studies demonstrate that LGR5-expressing supporting cells, which retain stem cell features, have the capability to differentiate into hair cells *in vitro* (Bramhall et al., 2014; Chai et al., 2012; Li et al., 2015; Shi et al., 2012). Therefore, understanding of mammalian hair cell differentiation mechanism and discovery of effective stimulators for hair cell generation are crucial for potential therapies of hearing loss.

Over the past two decades, a number of genes and signaling pathways have been reported to regulate inner ear hair cell development (Chai et al., 2012; Dabdoub et al., 2008; Gnedeva and Hudspeth, 2015; Golden et al., 2015; Huh et al., 2012; Kiernan, 2013; Kuo et al., 2015; Li et al., 2015; Mizutari et al., 2013; Ono et al., 2014; Shi et al., 2014). Of them, Notch signaling has been shown

to be a major player in the specification of prosensory epithelium and regulation of hair cell differentiation (Munnamalai et al., 2012; Pan et al., 2010). Activation of Notch signaling contributes to choosing the sensory progenitor fate and maintaining their undifferentiated status. Inactivation of Notch signaling in conditional knockout mouse models or by pharmacological inhibitors induces an increase in hair cell production (Kiernan, 2013; Li et al., 2015; Mizutari et al., 2013). Another important factor is MATH1, a basic-helix-loop-helix transcription factor. MATH1 is not only sufficient to induce differentiation of supporting cells into hair cells (Gao, 2003; Shou et al., 2003; Zheng and Gao, 2000), but also required for hair cell differentiation (Bermingham et al., 1999; Woods et al., 2004). More recently, Liang et al. (2012) reported that in the zebrafish the signal transducer and activator of transcription 3 (STAT3) signaling, a classical pathway activated by extracellular factors (Tadokoro et al., 2014), plays a role in regulation of zebrafish neuromast hair cell development. The zebrafish lateral line neuromasts are similar to the mammalian inner ear sensory epithelium in structure. STAT3 signaling is activated following hair cell damages and hair cell regeneration in the lateral line neuromasts. Knock down of *Stat3* decreases the number of hair cells by downregulating *Math1* expression during hair cell development. However, the importance of STAT3

signaling for mammalian inner ear hair cell differentiation and the relationship between STAT3 and Notch signaling pathways during this process are still unknown.

On the other hand, normal tissue homeostasis is maintained through symmetric and asymmetric cell divisions of stem/progenitor cells (Knoblich, 2010; Yang et al., 2015). Symmetric divisions are required for the expansion of progenitor numbers, while asymmetric divisions are operated to give rise to differentiated cells. For instance, in developing prostates, basal cells display symmetric division to produce daughter cells with self-renewal capacity, and undergo asymmetric division to generate daughter cells to achieve both self-renewal and differentiation potential (Wang et al., 2014). Up to now, the cell division modes that the inner ear supporting cells undergo have never been examined and whether STAT3 signaling influences these cell division modes during hair cell differentiation has not been reported.

In this study, we report that STAT3 activation is specifically correlated with hair cell differentiation. Either conditional *Stat3* gene deletion in mice *in vivo* or pharmacological inhibition of the STAT3 pathway *in vitro* leads to a decreased production of hair cells. Such effects appear to be achieved by shifting from asymmetric divisions to symmetric divisions of supporting cells. In addition, STAT3 signaling is activated when the Notch pathway is inhibited by either using *Notch1* conditional knockout mice or administration with a pharmacological inhibitor, and blocking STAT3 signaling attenuates the effect of the inhibition of Notch signaling on induction of extra hair cells. Thus, STAT3 signaling is an important regulator of hair cell differentiation in mammalian cochleae.

RESULTS

STAT3 Is Selectively Expressed and Activated in the Prosensory Epithelium of the Developing Mouse Cochlea *In Vivo*

To determine expression patterns of STAT3 signaling molecules in the mouse inner ear epithelium, we performed qRT-PCR experiments of four STAT3 signaling-related genes, including *Jak1*, *Jak2*, *Stat3*, and *Socs3* (Liang et al., 2012). As shown in Figure 1A, *Stat3* showed a relatively high expression level in the cochlea relative to the other three genes at post-natal day 0 (P0). Temporally, the *Stat3* expression level was increased gradually during cochlear development from E14 to P0, but decreased at P5 and P15 (Figure 1B).

To get a better idea about the cellular expression patterns of STAT3 signaling molecules during hair cell development, we dissected, dissociated, and fluorescence-activated cell

sorting (FACS) sorted hair cells, non-hair cell epithelial cells, and mesenchymal cells from the developing inner ear tissues prepared from the *Math1-GFP* transgenic mice, in which *Math1* is the promoter driving the reporter GFP (Woods et al., 2004). In addition to separate hair cells by using green fluorescence, we also used VIMENTIN as a marker to separate epithelial versus mesenchymal cells (Figures S1A and S1B). The inner ear cells from *Math1-GFP* mice were divided into three groups: Hc (MATH1-GFP$^+$ hair cells), Ep (MATH1-GFP$^-$ epithelial cells), and Me (VIMENTIN$^+$ mesenchymal cells). qRT-PCR analysis showed that *Stat3* expression level was higher in Hc than that in Ep and Me groups (Figure 1C). To confirm the qRT-PCR data, we examined the exact spatial expression patterns of STAT3 in the cochlea by immunostaining the otocyst sections with an antibody against STAT3 at various development time points. At E11, the stage prior to sensory cell specification, a diffused expression of STAT3 was observed throughout the cochlear prosensory epithelium. However, at E14, there was a restricted expression of STAT3 in the prosensory epithelium region, in which progenitor cells just started to give rise to supporting cells and hair cells. Notably, STAT3 expression began to be at high levels in MYO7A$^+$ cells, which represent hair cells at E14, and was confined to hair cells at E18 and P0 as development progressed. At P5, STAT3 were expressed in the cochlea hair cells as well as a small fraction of supporting cells that were located surrounding the hair cells (Figure 1D).

To get more insight into the role of STAT3 signaling in hair cell development, we examined its activation by immunostaining with an antibody against phosphorylated STAT3 at serine 727 (STAT3 pS727). We found that expression of STAT3 pS727 was limited in the MYO7A$^+$ domain at E14, and maintained through all of the three turns of the cochlea at E14–P0 (Figure 1E). In addition, STAT3 and STAT3 pS727 were also expressed in hair cells within vestibular sensory organs including crista (Figures S2A and S2B). These expression patterns of STAT3 and STAT3 pS727 in the cochlea and vestibular organs imply that STAT3 is possibly engaged in prosensory epithelial specification and highly associated with hair cell differentiation during inner ear morphogenesis.

STAT3 Is Activated during Hair Cell Differentiation *In Vitro*

To provide further evidence that STAT3 signaling is associated with hair cell differentiation, we first performed non-adhesive cultures using FACS sorted GFP$^-$ inner ear supporting cells prepared from the *Math1-GFP* mice at E18 to form otospheres, and then transferred them to an adhesive substrate to generate newly differentiated hair cells (the latter is named as otosphere-adhesive differentiation
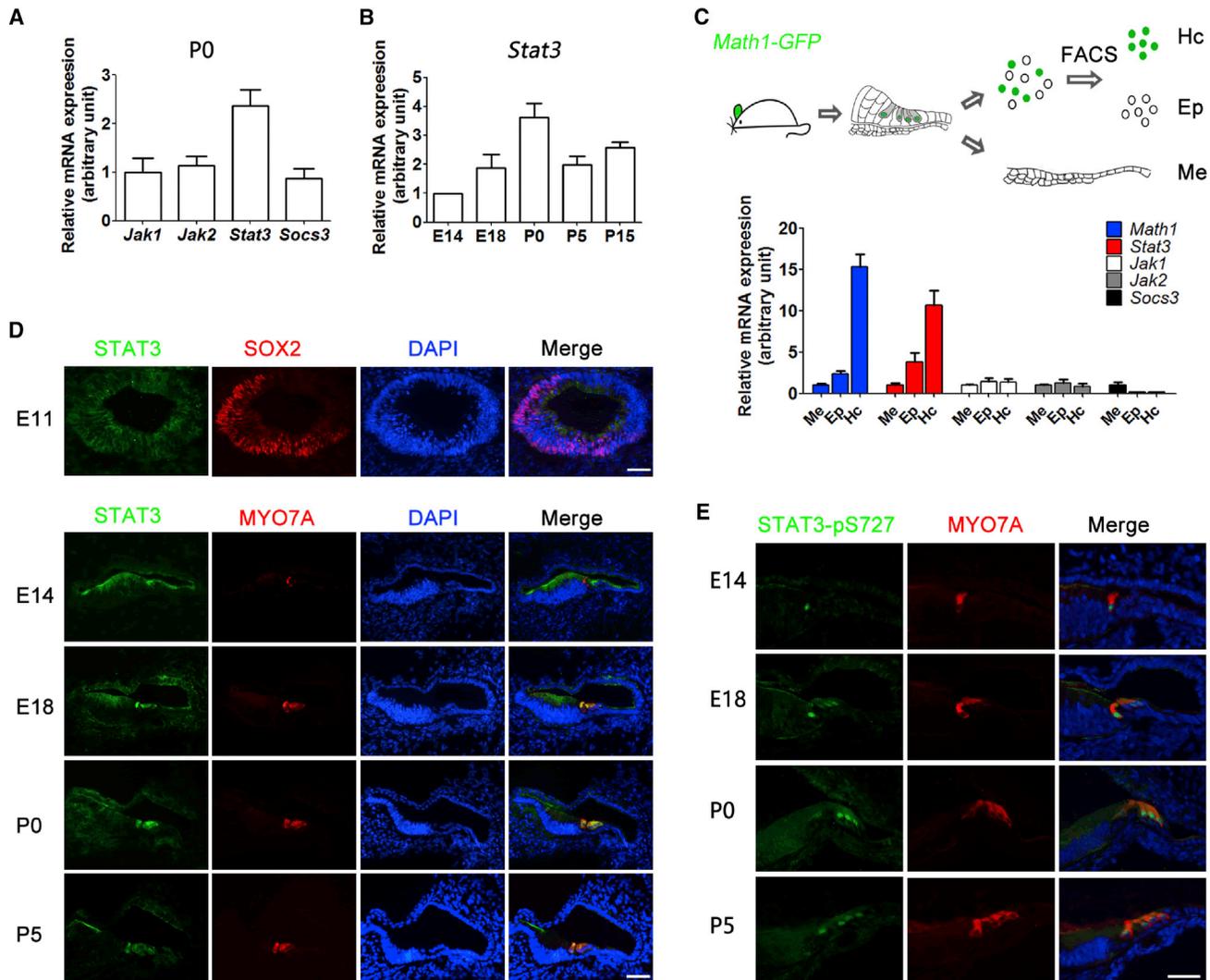
Figure 1. Expression Patterns of STAT3 in the Organ of Corti

(A) qRT-PCR analysis of relative *Jak1*, *Jak2*, *Stat3*, and *Socs3* mRNA levels in the cochlea at P0 (n = 3 independent experiments).

(B) qRT-PCR analysis of *Stat3* mRNA expression in the cochlear epithelium at stages from E14 to P15 (n = 3 independent experiments).

(C) Schematic diagram of dissociated inner ear cells from *Math1-GFP* mice. See Figures S1A and S1B for verification of supporting cell purification from *Math1-GFP* mice. qRT-PCR data of *Math1*, *Stat3*, *Jak1*, *Jak2*, and *Socs3* mRNA levels in hair cells (Hc), non-hair cells epithelia (Ep), and mesenchymal cells (Mc), respectively.

(D) Immunohistochemistry results using anti-STAT3, anti-SOX2, or anti-MYO7A antibodies on the cochlear section at E11, E14, E18, P0, and P5. Scale bar, 100 μm.

(E) Immunohistochemistry analysis for STAT3 pS727 and MYO7A at the stages from E14 to P5. Scale bar, 100 μm.

cultures). By taking advantage of *Math1-GFP* mice in which all hair cells are GFP positive in the cochlea, hair cells could be easily sorted by FACS. Supporting cells, expressing SOX2 but not MATH1-GFP or VIMENTIN (Figures S1A and S2B), were sorted out by FACS as described previously (White et al., 2006). Under otosphere-adhesive differentiation culture, spontaneous hair cell differentiation occurred as the newly formed hair cells expressed MATH1-GFP and MYO7A (Figure 2A). We found that STAT3 was highly ex-

pressed in the newly differentiated hair cells as they were MATH1-GFP positive and MYO7A positive by immuno-staining assay (Figure 2B). Importantly, we also observed phosphorylated STAT3 (STAT3 pS727 and STAT3 pY705) in the newly produced hair cells (Figures 2C and 2D), indicating that STAT3 activation was involved in hair cell fate determination. qRT-PCR assay showed that, adhesive otosphere cells displayed an increased mRNA level of *Stat3*, concomitant with upregulated expression of *Math1*, as hair
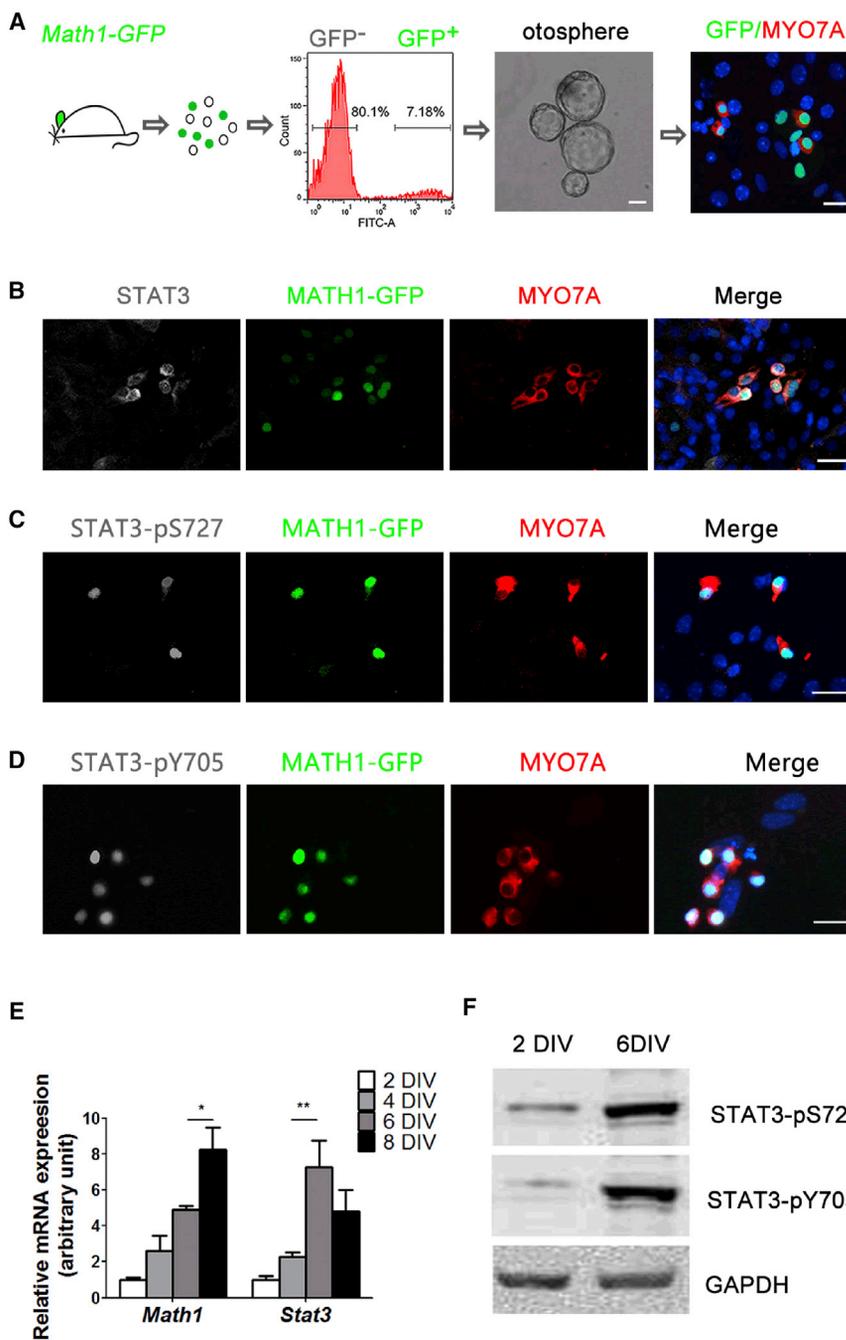
Figure 2. STAT3 Activation during Hair Cell Differentiation *In Vitro*

(A) Schematic drawings of hair cell generation from *Math1-GFP* mice *in vitro*. Scale bar, 20 μm.

(B–D) Immunostaining for STAT3, STAT3 pS727, STAT3 pY705, and Myo7a expression and cellular localization during hair cell differentiation. Scale bar, 20 μm.

(E) qRT-PCR data of *Math1*, *Stat3* mRNA expression in otosphere-adhesive differentiation cultures at 2 to 8 DIV (n = 3 independent experiments).

(F) Immunoblot of STAT3 pS727, STAT3 pY705, and STAT3 at 2 and 6 DIV, respectively. GAPDH is used as a loading control. Mean ± SEM; Student's t test; *p < 0.05, **p < 0.01.

cell differentiation proceeded (Figure 2E). Immunoblotting results showed that STAT3 pS727 and STAT3 pY705 levels were both higher at 6 days *in vitro* (DIV) than that at 2 DIV during hair cell differentiation (Figure 2F). Thus, otosphere-adhesive differentiation cultures re-capitulated what was observed in the developing inner ear *in vivo*, that is, STAT3 signaling was activated in the process of hair cell differentiation and positively correlated with *Math1* expression in a stage-dependent manner.

Deletion of the *Stat3* Gene Leads to Defects in Mouse Cochlear Hair Cell Development *In Vivo*

To determine whether the *Stat3* gene is functionally crucial for cochlear sensory epithelial development *in vivo*, we generated a *Sox2CreER;Stat3^flox/flox^* mouse line in which *Stat3* can be deleted following induction of Cre activity by continuously treating pregnant mice from E13 to E15 with tamoxifen (Figure 3A) as SOX2 is a selective prosensory epithelial cell marker in the otocyst (Dabdoub et al.,
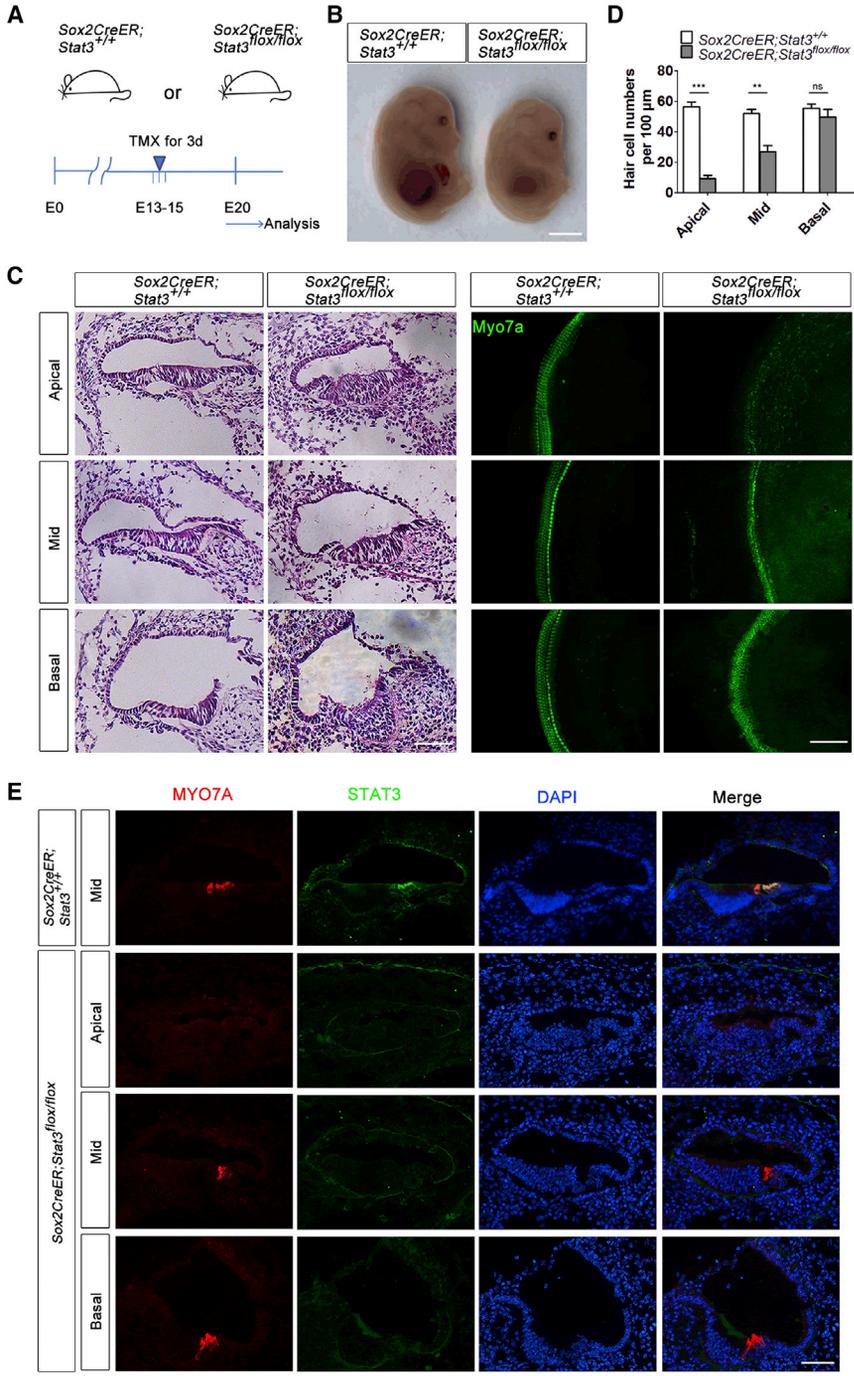
(A) Schematic illustration and the time course of Cre-inducible activity *in vivo*. Knock out of *Stat3* was induced beginning at E13.

(B) Representative embryos from *Sox2CreER; Stat3+/+* (*WT*) and *Sox2CreER;Stat3flox/flox* (*Stat3 CKO*) mice are presented. Scale bar, 500 μm.

(C) H&E staining analysis of cochlear sections from *Sox2CreER;Stat3+/+* and *Sox2CreER; Stat3flox/flox* mice. Immunohistochemistry for MYO7A expression in cochlear explants. Scale bar, 100 μm.

(D) Quantification of MYO7A+ hair cells in cochlear explants (n = 6 different cochlea).

(E) Immunostaining for STAT3 and MYO7A in different cochlear turns. Scale bar, 100 μm. Mean ± SEM; Student's t test; **p < 0.01, ***p < 0.001.

2008). Although *Sox2CreER;Stat3flox/flox* mice showed postnatal lethality, we were able to examine their cochlear phenotypes by dissecting and examining the embryonic tissues. As shown in Figure 3B, the cochlear phenotypes were analyzed at E20, *Sox2CreER;Stat3flox/flox* (*Stat3 CKO*) mouse was smaller in size and showed microcephaly relative to *Sox2CreER;Stat3+/+* (*WT*) mouse. Histology of the cochlea at E20 exhibited disorganization of supporting cells

and hair cells in *Stat3 CKO* cochleae, while *WT* mice showed a normal cochlear structure, regular structural arrangement of the sensory epithelium, and a developmental pattern (Figure 3C). *Stat3* deletion was confirmed by immunostaining with STAT3 antibody in otic vesicle tissue section of *Stat3 CKO* mice (Figure 3E). Immunostaining for MYO7A from isolated cochlear explants indicated that, compared with *WT* mice, *Stat3 CKO* mice displayed a

significant reduction in the number of hair cells. We divided cochlear turns into three parts and counted the number of MYO7A⁺ hair cells. Decreases of 83%, 48%, and 10% were observed in hair cell number in the apical, mid, and basal turns, in *Stat3 CKO* versus control littermates, respectively, indicating that the hair cell loss due to deletion of *Stat3* was more severe in the apical turn than that in the basal turn (Figure 3D). Immunofluorescence results from *Stat3 CKO* cochlear sections showed similar results: sections from the apical turn had no MYO7A⁺ hair cell, the middle turn showed one inner hair cell and two outer hair cells (OHCs), and the basal turn showed four regular hair cells (Figure 3E). Notably, *Stat3 CKO* mice received tamoxifen administration from E16 to E18 displayed a milder reduction in the number of MYO7A⁺ hair cells, and *Stat3 CKO* mice subjected to tamoxifen administration from P0 to P3 had no significant effect on hair cell production (Figure S4). These results indicated that inactivation of STAT3 appears to affect hair cell differentiation only at the early developmental stage. *Stat3 CKO* mice also showed a reduction in the number of CALRETININ⁺ cells, which also represent hair cells (Figure S3A). qRT-PCR study showed downregulated levels of hair cell-related genes in *Stat3 CKO* mice, including *Math1*, *Myo7a*, *Pou4f3*, and *Gfi1* (Figure S3B). In addition, *Stat3 CKO* mice displayed increased expression of Notch-downstream genes, *Hes5* and *HeyL*, which are negatively associated hair cell differentiated (Doetzlhofer et al., 2009) (Figure S3C). In addition, absence of STAT3 in the sensory epithelium affects neural connection with spiral ganglion cells, as revealed by a dramatic loss of TUJ1 and MAP2 expression in the *Stat3 CKO* mice (Figures S3D and S3E), indicating a neuronal innervation defect due to hair cell loss induced by *Stat3* deletion. These data together demonstrate that loss of STAT3 signaling impairs hair cell differentiation and functions during inner ear development *in vivo*.

Inactivation of STAT3 Impedes Hair Cell Differentiation *In Vitro*

To assess the effects of STAT3 signaling on hair cell production *in vitro*, we first performed *Sox2CreER;Stat3⁺/⁺* (WT) and *Sox2CreER;Stat3ᶠˡᵒˣ/ᶠˡᵒˣ* (*Stat3 CKO*) cochlear explant cultures in the presence of 4-OH tamoxifen to induce Cre activity. We explanted cochlea at E14 and cultured them for 7 days, which recapitulates the process of hair cell differentiation (Figure 4A). Consistent with loss-of-function studies *in vivo*, the number of MYO7A⁺ cells was decreased significantly in *Stat3 CKO* cochlear explants at E14. The apical-mid turn of cochlear explants showed a significant loss of hair cell compared with the explants from mid-basal turn. On the contrary, there was no change of hair cell numbers in *WT* explants after exposure
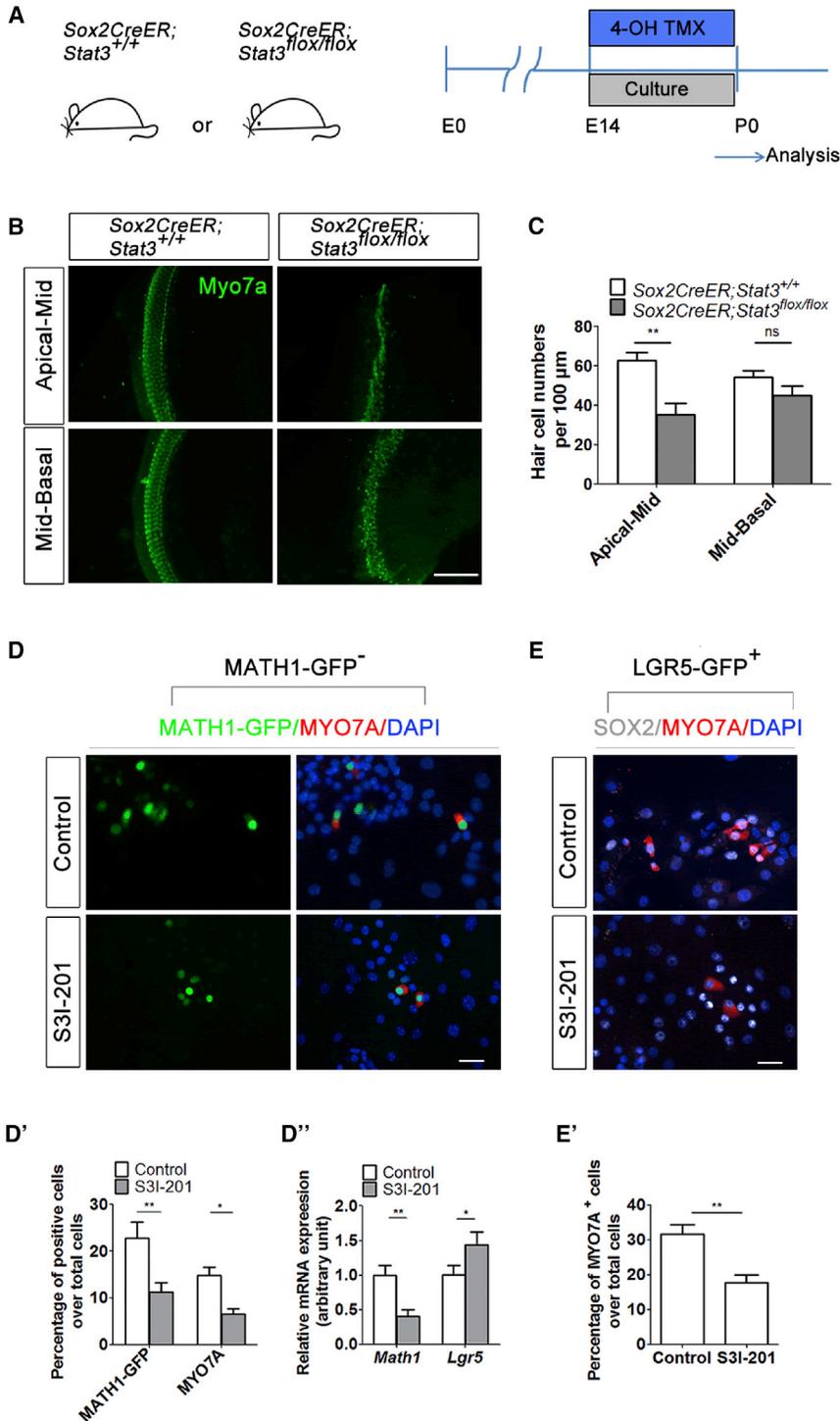
to 4-OH tamoxifen (Figures 4B and 4C). In addition, when a well-known STAT3 inhibitor, S3I-201, was added to the otosphere-adhesive differentiation culture to suppress STAT3 activation, the number of MATH1-GFP⁺ cells and MYO7A⁺ cells was reduced remarkably compared with that in control cultures (Figure 4D and 4D′). qRT-PCR analysis revealed that S3I-201 dramatically suppressed expression of *Math1*, and increased expression of *Lgr5* (Figure 4D″).

Given the fact that LGR5 has recently been shown to be a more authentic hair cell progenitor marker (Bramhall et al., 2014; Chai et al., 2012; Li et al., 2015; Shi et al., 2012), we decided to determine whether inhibition of the STAT3 signaling also impedes hair cell production derived from the LGR5-expressing supporting cells. First, we employed *Lgr5-EGFP-IRES-CreER* (referred as *Lgr5-GFP*) mice to purify LGR5⁺ supporting cells (LGR5-GFP⁺/MYO7A⁻ cells) by FACS (Figure S1C) and then performed otosphere-adhesive differentiation cultures. S3I-201 application also decreased the production of MYO7A⁺ hair cells that are differentiated from LGR5-GFP⁺ cells (Figures 4E and 4E′). Thus, these experiment reinforce the conclusion that inactivation of STAT3 signaling inhibits hair cell differentiation.

STAT3 Signaling Regulates Cell Division Modes of Supporting Cells

To understand possible mechanisms by which STAT3 signaling modulates supporting cell differentiation, we performed experiments to examine cell division patterns during hair cell production in the otosphere-adhesive differentiation cultures. We performed 48-hr bromodeoxyuridine (BrdU) incorporation at different culture stages during hair cell differentiation (Figures 5A and S5A). As shown in Figures 5B and 5C, when BrdU pulse labeling was performed at the earlier time point (1–3 DIV) of the 9-day culture period, S3I-201 treatment increased BrdU⁺/SOX2⁺ and BrdU⁺/PROX1⁺ cell numbers in the cultures prepared from WT supporting cells, but decreased BrdU⁺/MATH1-GFP⁺ cell number prepared from MATH1-GFP⁻ supporting cells. Similar results were obtained in the cultures prepared from LGR5-GFP⁺ supporting cells (Figure 5B″). In addition, BrdU pulse labeling at 3–5 DIV showed an increase in BrdU⁺/SOX2⁺ and BrdU⁺/PROX1⁺ cell numbers, and a reduction in BrdU⁺/MATH1-GFP⁺ cell numbers. However, labeling at 5–7 or 7–9 DIV did not display much difference, possibly due to the fact that the overall cell proliferation is limited in the culture after 5–9 days (Figures S5B–S5D). Thus, inactivation of STAT3 leads to an expansion of supporting cells and decreases numbers of hair cells that are derived from the dividing supporting cells.

Next, to better understand the cellular mechanism related to mitosis-mediated production of hair cells and

expansion of supporting cells, we performed double immunostaining for SURVIVIN or α-TUBULIN to label the midbody to define anaphase/telophase of mitosis and for progenitor cell or differentiated cell markers to analyze the fates of two future daughter cells derived from the supporting cell. This type of study is also called cell division mode analysis (Wang et al., 2014). As shown in Figure 5D, there were three cell division modes: (1) both daughter cells expressing SOX2 were symmetrically segregated into two daughter cells when a progenitor/supporting cell divided (symmetric self-renewal, SOX2⁺/SOX2⁺ division); (2) when SOX2 was asymmetrically distributed into two
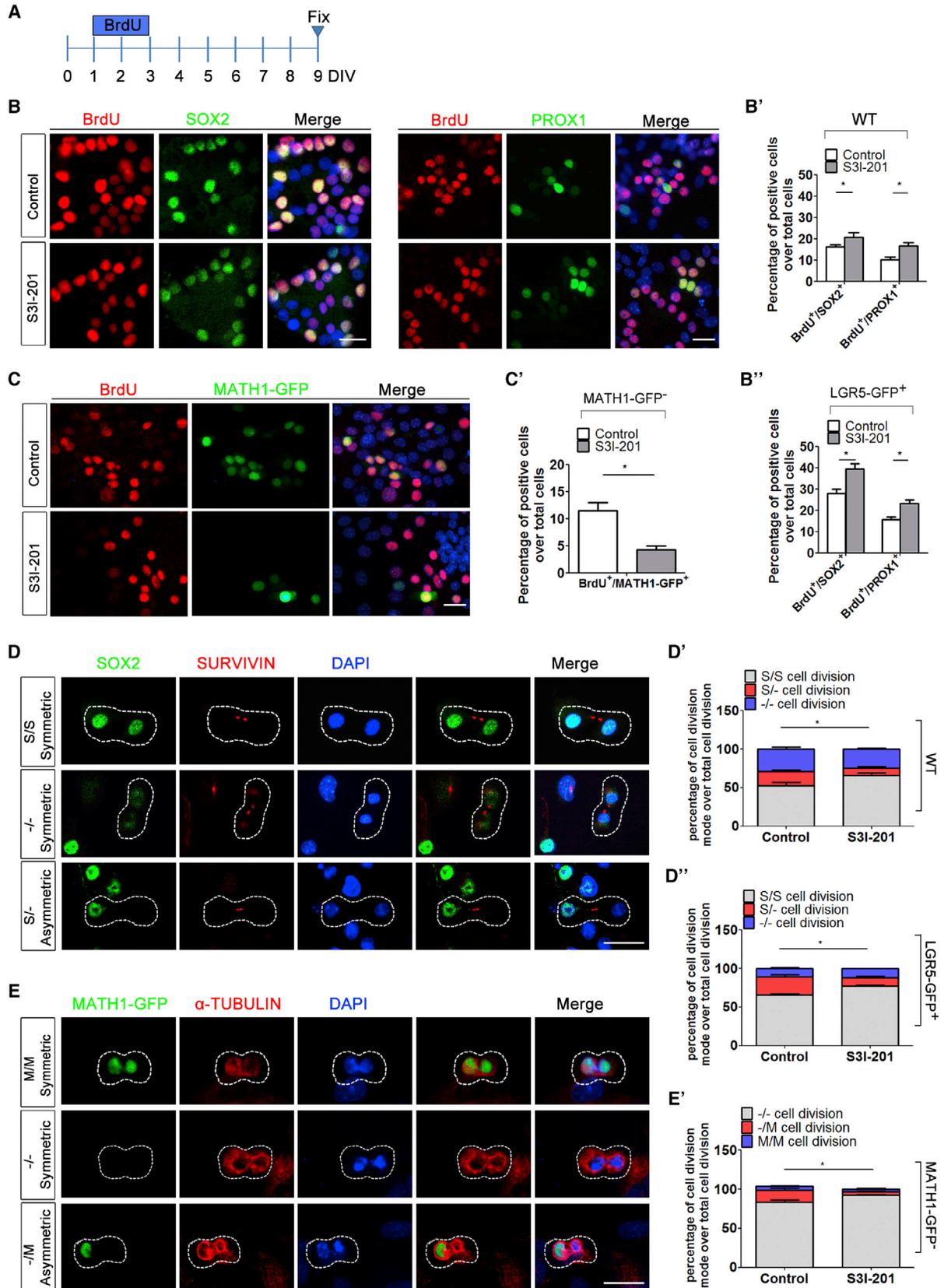
(legend on next page)

daughter cells (asymmetric division, SOX2$^+$/SOX2$^-$ division); (3) when SOX2 expression was lost in both daughter cells (symmetric commitment, SOX2$^-$/SOX2$^-$ division). We also further confirmed this event by analyzing daughter cells prepared from MATH1-GFP$^-$ supporting cells (Figure 5E). The supporting cell could either undergo a symmetric self-renewal to generate two MATH1-GFP$^-$ daughter cells (MATH1-GFP$^-$/MATH1-GFP$^-$ division) or symmetric commitment (MATH1-GFP$^+$/MATH1-GFP$^+$ division), which generated two MATH1-GFP$^+$ hair cells. In addition, a supporting cell underwent an asymmetric division to produce one daughter cell that was MATH1-GFP$^-$ and the other was MATH1-GFP$^+$ (MATH1-GFP$^-$/MATH1-GFP$^+$ division). To provide additional evidence for asymmetric and symmetric division modes, we also tested for the distribution of PROX1 (another supporting cell marker) and NUMB (another putative differentiated cell marker) (Kechad et al., 2012). Our immunostaining for NUMB revealed that it was expressed at high levels in MYO7A$^+$ hair cells, but low levels in LGR5-GFP$^+$ supporting cells (including pillar, Deiters', and inner phalangeal cells) (Figure S5F), supporting the notion that NUMB could be used as a differentiated cell marker to analyze symmetric and asymmetric divisions of the epithelial progenitor cells. As shown in Figure S5E, these two markers also displayed existence of symmetric and asymmetric division modes.

We then treated the cultured cells with S3I-201, to study its impact on the three models of cell divisions. Immunostaining for SOX2 revealed that about 9.8% of supporting cells went through asymmetric divisions in response to S3I-201, lower than that in the control group (18.5% ± 2.1%). Meanwhile, 65.6% ± 3.1% of supporting cells displayed symmetric self-renewal following treatment with S3I-201, higher than that in control group (52.2% ± 4.4%) (Figure 5D'). Analysis of SOX2 distribution between two daughter cells in the cultures prepared from LGR5-GFP$^+$ supporting cells showed similar results (Figure 5D''). Next, we investigated MATH1-GFP inheritance during hair cell differentiation *in vitro* using MATH1-GFP$^-$ supporting cells. S3I-201 treatment showed a reduced ratio of asymmetric divisions of supporting cells, but an enhanced ratio of symmetric self-renewal divisions (Figure 5E'). To confirm this, we also assessed self-renewal capacity in the absence of STAT3 signaling pathway by performing otosphere experiments. S3I-201 administration promoted formation of otosphere in both numbers and sizes (Figures S6A and S6B). Similar results were seen in the cell cultures prepared from *Stat3 CKO* mice (Figures S6C and S6D). Therefore, the interference of STAT3 broke the balance of cell division modes by shifting from asymmetric divisions to symmetric divisions to diminish hair cell production.

Inhibition of Notch Signaling Induces STAT3 Phosphorylation

To further investigate the mechanism of STAT3 signaling during prosensory epithelia cell differentiation, we paid our attention to Notch signaling as the latter is so far the most important pathway in regulation of the inner ear sensory cell fate (Kiernan, 2013; Li et al., 2015; Mizutari et al., 2013; Pan et al., 2010). First, we checked whether the effects of STAT3 signaling on determination of sensory cell fates were correlated with the Notch signaling activity. *Sox2CreER;Notch1$^{flox/flox}$ (Notch1 CKO)* mice were utilized to inactivate Notch signaling when Cre was activated by administration with tamoxifen from E14 to E16, and the cochlear phenotypes were then analyzed at P0 (Figure 6A). In agreement with previous reports (Li et al., 2015), *Notch1 CKO* mice exhibited an increase in MYO7A$^+$ hair cell numbers. Notably, STAT3 and STAT3 pS727 were also expressed in ectopic hair cells (Figure 6B). In addition,

Figure 5. Inhibition of STAT3 Reduces Asymmetric Divisions
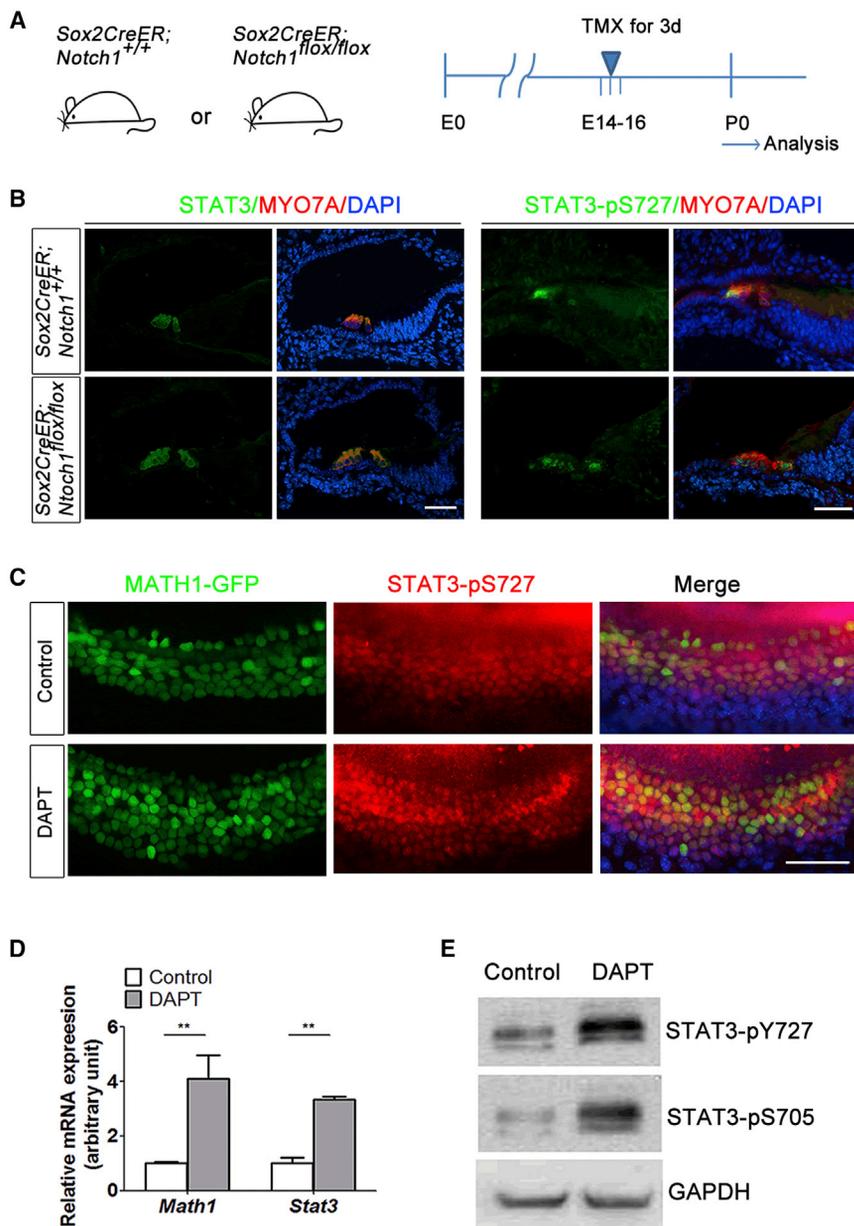(A) Schematic illustration of BrdU incorporation in otosphere-adhesive differentiation culture.
(B) Immunostaining for BrdU together with Sox2 or Prox1 in control or S3I-201-treated groups. Scale bar, 20 μm. (B' and B'') Quantification of BrdU$^+$/SOX2$^+$ cells or BrdU$^+$/PROX1$^+$ cells in the cultures prepared from WT (B') or LGR5-GFP$^+$ supporting cells (B'') in the presence or absence of S3I-201. (n = 3 independent experiments).
(C) Immunostaining for BrdU with MATH1-GFP and (C') quantification of BrdU$^+$/MATH1-GFP$^+$ cells from MATH1-GFP$^-$ supporting cells in control and S3I-201 groups (n = 3 independent experiments). Scale bar, 20 μm.
(D) Immunodetection of division models of a dividing cell in anaphase/telophase using anti-SOX2 and SURVIVIN antibodies. The outline indicates a dividing cell. Scale bar, 20 μm. (D'-D'') Statistical analysis of the percentage of different division modes (S/S, S/−, −/−) over the total cell divisions in the cultures prepared from WT (D') or LGR5-GFP supporting cells (D'') in the presence or absence of S3I-201 (n = 3 independent experiments). S/S:SOX2$^+$/SOX2$^+$ division (symmetric self-renewal); S/−:SOX2$^+$/SOX2$^-$ division (asymmetric division); −/−:SOX2$^-$/SOX2$^-$ division (symmetric commitment).
(E) Immunodetection of division modes using anti-α-TUBULIN antibody along with MATH1-GFP. Scale bar, 20 μm. (E') Statistical analysis of the percentage of different division modes (−/−, −/M, M/M) over the total cell divisions in the cultures prepared from MATH1-GFP$^-$ supporting cells in the presence or absence of S3I-201 (n = 3 independent experiments). −/−:MATH1-GFP$^-$/MATH1-GFP$^-$ division (symmetric self-renewal); −/M:MATH1-GFP$^-$/MATH1-GFP$^+$ division (asymmetric division); M/M:MATH1-GFP$^+$/MATH1-GFP$^+$ division (symmetric commitment).
Mean ± SEM; Student's t test; *p < 0.05.

Figure 6. Inhibition of Notch Signaling Pathway Induces STAT3 Activation

(A) Schematic illustration and the time course of inducible Cre activity *in vivo*. Deletion of *Notch1* was induced beginning at E14.

(B) Immunostaining for STAT3, STAT3 pS727, and MYO7A in *Sox2CreER;Notch1*^{+/+} and *Sox2CreER;Notch1*[flox/flox] cochlear sections. Scale bar, 100 μm.

(C) Immunostaining for STAT3 pS727 antibody along with MATH1-GFP in control and DAPT-treated groups. Scale bar, 100 μm.

(D and E) qRT-PCR analysis of *Math1, Stat3* mRNA levels and Immunoblotting of STAT3 pS727, STAT3 pY705 in control and DAPT-treated explant cultures (n = 6 different cochlea). GAPDH is used as a loading control. Mean ± SEM; Student's t test; **p < 0.01.

we also observed enhanced STAT3 activity when Notch signaling was pharmacologically abolished by DAPT, which blocks the Notch ligand-dependent cleavage and activation of Notch receptors (Mizutari et al., 2013) in the cochlear explant cultures. Immunostaining analysis on the explant cultures revealed an increase in STAT3 pS727 levels in parallel to production of an extra number of hair cells (Figure 6C). Similarly, immunoblot analysis of cochlear explants showed that, accompanied by Notch inactivation, both STAT3 pY705 and STAT3 pS727 expression were significantly upregulated (Figure 6E). In addition, qRT-PCR study also showed an upregulation of *Stat3* expression in the *Notch1 CKO* cochlear but not in the *WT*

tissues (Figure 6D). These finding suggest that perturbing Notch signaling may activate STAT3 signaling in the sensory epithelia.

STAT3 Activation Appears to Partially Mediate Hair Cell Production Induced by a NOTCH Pathway Inhibitor

Given that Notch inhibition promotes the phosphorylation of STAT3, we hypothesized that the inhibitory effect of Notch signaling on sensory cell development might be partly achieved through STAT3 activation. To substantiate this hypothesis, we performed otosphere-adhesive differentiation cultures in the presence of DAPT or S3I-201, or
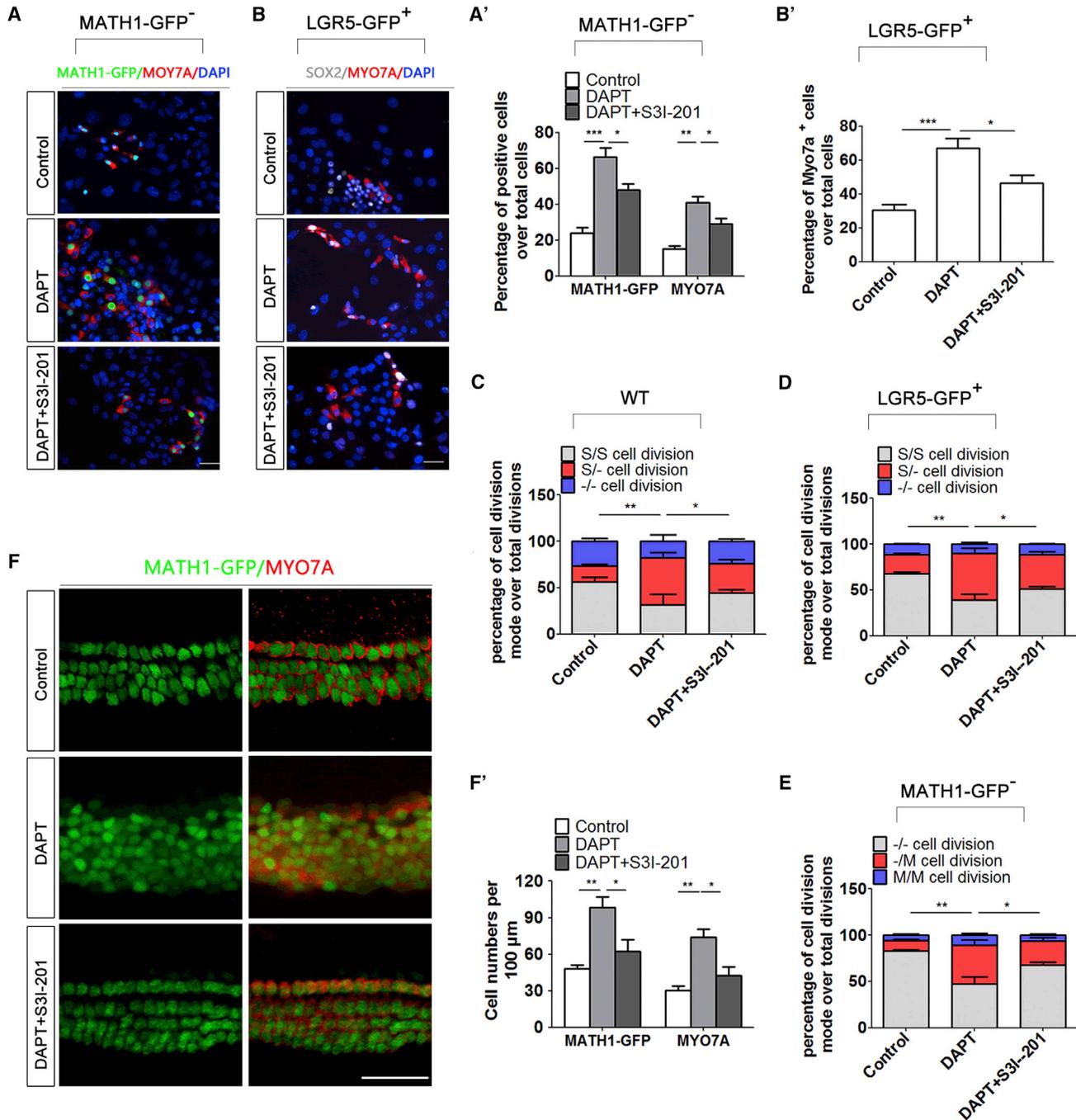
Figure 7. Crosstalk between STAT3 and Notch Signaling Pathways during Hair Cell Differentiation

(A) Immunostaining with MYO7A antibody along with MATH1-GFP. Scale bar, 20 μm. (A') Quantitation of MATH1-GFP⁺/MYO7A⁺cells in the culture prepared from MATH1-GFP⁻ supporting cells in the absence or presence of DAPT, or DAPT together with S3I-201 (n = 3 independent experiments).

(B) Immunostaining for SOX2 and MYO7A. Scale bar, 20 μm. (B') Quantification of MYO7A⁺ cells in the cultures prepared from LGR5-GFP⁺ supporting cells in the absence or presence of DAPT, or DAPT together with S3I-201 (n = 5 independent experiments).

(C–E) Statistical analysis of the percentage of different division modes over total cell divisions in the cultures prepared from WT (C), LGR5-GFP⁺ (D), and MATH1-GFP⁻ supporting cells (E) in the absence or presence of DAPT or DAPT together with S3I-201 (n = 3 independent experiments).

(legend continued on next page)

both. Consistent with previous reports (Doetzlhofer et al., 2009; Mizutari et al., 2013), inhibition of Notch signaling by DAPT led to an increase in MATH1-GFP$^+$ and MYO7A$^+$ cell numbers. When S3I-201 was added to the cultures along with DAPT, the increase in the number of MATH1-GFP$^+$ and MYO7A$^+$ cells was diminished (Figures 7A and A′). In addition, analysis of MYO7A$^+$ cells differentiated from LGR5-GFP$^+$ supporting cells showed similar results (Figures 7B and 7B′). These data together indicate that DAPT causes an increase in hair cell numbers during hair cell differentiation, while S3I-201 reverses the effects induced by DAPT.

To determine whether cell division mode change induced by STAT3 activation also mediates hair cell production induced by inhibition of Notch signaling, we performed BrdU immunostaining and cell division mode analysis in the otosphere-adhesive differentiation cultures. DAPT treatment decreased BrdU$^+$/SOX2$^+$ and BrdU$^+$/PROX1$^+$ cell numbers, but increased BrdU$^+$/MATH1-GFP$^+$ cell numbers, showing an increase in mitosis-derived production of hair cells after Notch signaling was blocked. Application of S3I-201 along with DAPT reduced mitosis-derived generation of hair cells to attenuate the Notch inhibition-dependent effects (Figures S7A–S7A″). Analysis of SOX2 segregation in the two daughter cells displayed that 50.4% ± 5.4% supporting cells went through asymmetric division in response to DAPT, which was much higher than that in the control group. The proportion of supporting cells undergoing symmetric self-renewal divisions after administration with DAPT (31.8% ± 10.2%) was much lower than that in the control group (Figure 7C). Quantification of SOX2 distribution between two daughter cells generated from LGR5-GFP$^+$ supporting cells (Figure 7D) or MATH1-GFP distribution prepared from MATH1-GFP$^-$ supporting cells (Figure 7E) showed similar results. Taken together, blockade of Notch signaling induced a shift to more asymmetric divisions in supporting cells to promote production of more daughter hair cells. However, after exposure to S3I-201 in combination with DAPT, supporting cells reversed cell division modes induced by Notch inhibition via a change from asymmetric divisions to symmetric divisions (Figures 7A–7E).

Next, we explored the relationship between Notch and STAT3 signaling on the production of hair cells in cochlear explant cultures. When exposed to DAPT, the explants showed production of supernumerary MATH1-GFP$^+$ and MYO7A$^+$ hair cells, leading to excess of the hair cell differentiation, compared with the control cultures. Addition of S3I-201 along with DAPT abolished generation of ectopic hair cells, as seen by a restoration of a relatively normal number of hair cells (Figure 7F and 7F′). qRT-PCR study showed a downregulation of *Hes5* and *HeyL* in the presence of DAPT, while S3I-201 reversed this effect (Figure S7B). In addition, imaging acquisition of the cochlear explants cultures at different time points revealed that S3I-201 weakened the hair cell production effect by DAPT in a time-dependent fashion, when the cultures were treated together with DAPT and S3I-201 (Figures S7C and S7D). Thus, suppression of STAT3 signaling reverses the effects of blocking the Notch pathway on hair cell differentiation.

DISCUSSION

Using conditional *Stat3* and *Notch1* knockout mouse models and pharmacological STAT3 and Notch pathway inhibitors in otosphere-adhesive differentiation or cochlear explant cultures, the present study provides evidences for a role of STAT3 signaling in supporting cell proliferation and hair cell differentiation in mammalian cochleae. In addition, by studying cell division modes of supporting cells during normal development and inactivation of Notch signaling-induced production of supernumerary hair cells, our experiments also shed additional light onto cellular and molecular mechanism regarding how STAT3 signaling regulates mammalian inner ear hair cell differentiation.

The Role of STAT3 Signaling in Hair Cell Development
The specification of sensory cells is believed to be attributed to the spatiotemporal expression levels of determinants in developing cochlear epithelia (Ono et al., 2014). In the present study, we found that STAT3 and STAT3 pS727 were confined selectively in hair cells in the inner ear. Conditional knock out of STAT3 in the sensory domain resulted in a disorganization of the cochlear epithelium, inhibition of hair cell development, and a significant downregulation of hair cell-related genes. Our findings are consistent with previous reports on a role of STAT3 signaling in zebrafish lateral line neuromast formation based on a powerful transcriptional profiling of gene expression (Liang et al., 2012).

The role of STAT3 signaling in the mouse inner ear appears to development dependent. When STAT3 signaling was disrupted at E13, a time point at which hair cell generation is just starting, cochlear explants showed an obvious deficit in hair cell numbers. However, cochlear deletion of

---

(F) Immunostaining for MYO7a together with MATH1-GFP on cochlear explants. Scale bar, 100 μm. (F′) Quantitation of MATH1-GFP$^+$/MYO7A$^+$ cell numbers in the control group versus the groups treated with DAPT or DAPT together with S3I-201 (n = 3 independent experiments).
Mean ± SEM; Student's t test; *p < 0.05, **p < 0.01, ***p < 0.001.

Stat3 induced at E16 or P0 exhibited only mild or no obvious defects in hair cell formation, respectively, indicating that the impact of *Stat3* deletion is more severe at the early stage of hair cell development. Consistently, inhibition of hair cell differentiation, caused by lack of STAT3 signaling in the sensory epithelium, was more prominent in the apical turn than the basal turn of the cochlea explant, due to a development gradient from the basal-to-apical turn. In addition, deletion of *Stat3* also led to a more severe reduction in the number of OHCs, but not much effect on IHCs. Considering that previous studies have shown that HES5 expression is essential for differentiation of OHCs, while HES1 is critical for production of IHCs (Zheng et al., 2000; Zine et al., 2001), this raises a possibility that HES5 deficiency might be a mechanism underlying the OHCs deficit seen in the *Stat3 CKO* mice. Consistent with this notion, our qRT-PCR analysis indeed demonstrated a downregulation of *Hes5* in the *Stat3 CKO* mice.

It is worth mentioning that the hair cell phenotypes of *Stat3 CKO* mice resemble those in fibroblast growth factor (FGF) knockouts, indicating a requirement of the gene network for regulating hair cell differentiation (Huh et al., 2012; Munnamalai et al., 2012; Ono et al., 2014). Toward that direction, the FGF-STAT3 signaling pathway is reported to regulate cell-cycle exit and control neural crest specification (Nichane et al., 2010). The FGF receptor stimulates STAT3 phosphorylation in a GP130-dependent manner to promote breast tumorigenesis (Bohrer et al., 2014). Future studies are needed to investigate a possible mechanism regarding regulation of STAT3 by FGF in the process of hair cell differentiation.

Cell Division Mode Analysis during Hair Cell Differentiation

Stem cells achieve their self-renewal and differentiation via symmetric and asymmetric divisions (Knoblich, 2010; Wang et al., 2014; Yang et al., 2015). Understanding how the cell division modes are regulated is helpful to uncover the mechanism underlying stem cell proliferation and differentiation. Using double immunostaining for cell mitotic markers (SURVIVIN/α-TUBULIN) and supporting cell markers (SOX2/PROX1), or differentiated cell markers (MATH1-GFP/NUMB), the present experiments provided a useful method for studying cell division modes during hair cell generation. While SURVIVIN or α-TUBULIN staining helps to define the position of two future daughter cells, the supporting or differentiated cell markers identify the cell fates of daughter cells. Application of this method may allow us to identify crucial molecules that control cell division modes of sensory supporting cells and might provide therapeutic targets for stimulating inner ear supporting cell expansion or hair cell regeneration.

In this study, we found three cell division modes during hair cell differentiations, including symmetric self-renewal division, asymmetric division, and symmetric commitment division. Romero-Carvajal et al. (2015) have reported two patterns in regenerating hair cell from non-vertebrates that contain the amplifying cell division and the differentiating cell division. Our study may interpret these two patterns as follows: the amplifying cell division means symmetric self-renewal division, while the differentiating cell division indicates symmetric commitment. Notably, we discovered a distinct asymmetric division mode in addition to the two above-described modes, i.e., one daughter supporting cell and one daughter hair cell, suggesting an important cellular mechanism for production of hair cells. The beauty of this division mode is that it not only allows the production of hair cells, but also maintains the supporting cell numbers.

When the STAT3 pathway was blocked by S3I-201, the ratio of asymmetric divisions over the total cell divisions of supporting cells was reduced, and the rate of symmetric divisions of supporting cells was enhanced. Therefore, inhibition of STAT3 changes the balance of cell division modes by shifting from asymmetric divisions to symmetric divisions.

The Relationship between STAT3 and Notch Pathways

Given the findings that both STAT3 and Notch pathways play regulatory roles in inner ear development (Kiernan, 2013; Liang et al., 2012; Mizutari et al., 2013; Munnamalai et al., 2012), it is important to determine the relationship between these two pathways. Our study revealed that inhibition of the Notch pathway by either conditional knock out of the *Notch1* or a pharmacological inhibitor DAPT not only upregulated expression of STAT3, STAT3 pY705, and STAT3 pS727, but also increased the number of MATH1-GFP[+]/STAT3 pS727^{+} cells, implying that STAT3 activation might mediate the effects of inhibition of Notch on cochlear hair cell production. Consistent with this notion, recent work in other types of tissue, such as the lung airway epithelium (Tadokoro et al., 2014), confirms a negative relationship between Notch and STAT3 pathways. In this regard, inactivation of STAT3 signaling might tentatively attenuate the Notch inhibition-induced hair cell production effect. Our otosphere-adhesive differentiation and cochlear explant culture experiments provided supporting evidence for this hypothesis. Addition of S3I-201 together with DAPT into the cultures resulted in a counteraction on DAPT-dependent response, showing a regression of disordered epithelium, a recovery from the reduction in the hair cell numbers, and a reversion of the cell division modes.

Our observations that inhibition of the STAT3 pathway cannot completely reverse the differentiation-promoting

action of DAPT suggest that other factors might also be involved. For example, FGF signaling is a candidate regulator of Notch-STAT3-mediated action (Doetzlhofer et al., 2009; Munnamalai et al., 2012; Ono et al., 2014). Munnamalai et al. (2012) demonstrate that inactivation of Notch signaling downregulates FGF20 expression. FGF signaling is reported to control HEY2, and rescues the actions of disrupted Notch signaling on hair cell regeneration (Doetzlhofer et al., 2009). Whether, and how, STAT3 collaborates with other molecules such as FGF signaling to mediate the Notch inhibition-induced hair cell production remain to be studied.

In conclusion, STAT3 signaling is important for mammalian cochlear hair cell differentiation. It contributes to the downstream of the Notch pathway in regulation of hair cell production via influencing the balance between symmetric and asymmetric division modes of supporting cells.

EXPERIMENTAL PROCEDURES

Experimental Animals

Sox2-CreER, *Math1-GFP*, *Lgr5-EGFP-IRES-CreER* (referred as *Lgr5-GFP*), *Stat3*$^{flox/flox}$, and *Notch1*$^{flox/flox}$ mice were purchased from Jackson laboratory. For Cre activation, 100 μL tamoxifen (10 mg/mL, Sigma) was administered to pregnant mice via gavage. 4-OH tamoxifen (100 mg/L, Sigma) was added into medium to induce Cre activity *in vitro*. All mouse experiments were approved by the Institutional Animal Care and Use Committee at the School of Biomedical Engineering, Shanghai Jiao Tong University.

Cochlear Explant Cultures

The mice were anatomized at different stages after standard anesthesia. By careful removal of the stria vascularis, Reissner's membrane, and surrounding connective stroma, cochlear explants were separated in accordance with the method described previously (Zheng and Gao, 2000). Subsequently, explants were placed and cultured onto 6-well plates coated with rat tail collagen gels (50 μg/mL, BD Biosciences) in DMEM-F12 with B27 and N2 supplement (Invitrogen) for 7–10 days. The tissues were then fixed and immunostained for different markers.

Purification of Cochlear Cells

Cochlear explants were prepared from *Math1-GFP* or *Lgr5-GFP* mice according to the same protocol shown above. To dissect the sensory epithelium from non-sensory mesenchyme, we trypsinized the explants in DMEM/F12 with thermolysin (0.5 mg/mL, Sigma) and DNase (10 U/mL, Invitrogen) for 30–45 min at 37°C. After termination with DMEM containing 10% fetal bovine serum (Invitrogen), the separated sensory epithelial sheets were collected and then pipetted up and down gently. After being filtered through a 40-μm cell strainer, the cells were placed onto 12-well plates to obtain single cells. Employing a FACSAria cytometer (BD Biosciences), GFP$^+$ and GFP$^-$ cells were sorted out sequentially, both of which achieved >95% purity as immunostained by distinct markers. All the GFP$^+$, GFP$^-$, and mesenchymal cells were collected separately.

Otosphere-Adhesive Differentiation Cultures

To form otosphere, sorted cells as described above were placed at a clonal density (10 cells/μL) onto Ultra-Low Attachment dishes (Corning Life Sciences) and cultured in DMEM/F12 plus N2, B27 supplement, epidermal growth factor (20 ng/mL, R&D Systems), and FGF (10 ng/mL, R&D Systems). After 7–14 days, otospheres were collected and counted.

To analyze cell differentiation, we transferred otospheres onto plates coated with poly-D-ornithine (10 μg/mL, Invitrogen) and laminin (10 μg/mL, Invitrogen), which allow spheres to stick on the bottom. After adhesion, we changed the medium every 2 days, supplemented it with DMEM/F12, N2, and B27 factors, and cultured it for 7–10 days. For the hair cell differentiation generated from LGR5-GFP$^+$ supporting cells, it was noted that, after 7–10 days in culture, the green fluorescence of LGR5-GFP$^+$ supporting cells was lost, similar to studies by others (Chai et al., 2012; Shi et al., 2012).

Other Reagents

To determine if STAT3 signaling regulates hair cell differentiation, STAT3 inhibitor S3I-201 (10 μg/mL, Selleck) was added once the primary cells were seeded on dishes. For detection of mitosis cells, BrdU (10 μg/mL, Sigma) was added into medium during cell differentiation progress. The Notch inhibitor (γ-secretase inhibitor), DAPT (5 μM, Sigma), was used individually during culture period.

Cell Counting and Statistical Analysis

The cochlear explants and cells were distinguished using hair cell- and supporting cell-specific markers. Using the ImageJ software (NIH), we counted cells in the cochlear segments (100 μm) for each of the cochlear explants and those in 2,000 total cells for each of the otosphere-adhesive differentiation cultures, respectively. The quantitative data are presented as mean ± SEM. Statistical analyses were done with Student's t test.

SUPPLEMENTAL INFORMATION

Supplemental Information includes Supplemental Experimental Procedures, seven figures, and one table and can be found with this article online at http://dx.doi.org/10.1016/j.stemcr.2017.05.031.

AUTHOR CONTRIBUTIONS

W.-Q.G. and X.W. conceived the ideas and interpreted the results. Q.C. designed and conducted the major experiments. Y.Q., N.W., C.X., and Z.J. assisted in the cochlear explant cultures, FACS experiments, and data collection. H.H. and S.Y. helped discussions. Y.E.C., R.C., and H.L. provided or assisted in obtaining the reporter and CKO mice. Q.C. and W.-Q.G. wrote and revised the manuscript.

ACKNOWLEDGMENTS

REFERENCES

Bermingham, N.A., Hassan, B.A., Price, S.D., Vollrath, M.A., Ben-Arie, N., Eatock, R.A., Bellen, H.J., Lysakowski, A., and Zoghbi, H.Y. (1999). Math1: an essential gene for the generation of inner ear hair cells. Science *284*, 1837–1841.

Bohrer, L.R., Chuntova, P., Bade, L.K., Beadnell, T.C., Leon, R.P., Brady, N.J., Ryu, Y., Goldberg, J.E., Schmechel, S.C., and Koopmeiners, J.S. (2014). Activation of the FGFR–STAT3 pathway in breast cancer cells induces a hyaluronan-rich microenvironment that licenses tumor formation. Cancer Res. *74*, 374–386.

Bramhall, N.F., Shi, F., Arnold, K., Hochedlinger, K., and Edge, A.S. (2014). Lgr5-positive supporting cells generate new hair cells in the postnatal cochlea. Stem Cell Rep. *2*, 311–322.

Chai, R., Kuo, B., Wang, T., Liaw, E.J., Xia, A., Jan, T.A., Liu, Z., Taketo, M.M., Oghalai, J.S., and Nusse, R. (2012). Wnt signaling induces proliferation of sensory precursors in the postnatal mouse cochlea. Proc. Natl. Acad. Sci. USA *109*, 8167–8172.

Dabdoub, A., Puligilla, C., Jones, J.M., Fritzsch, B., Cheah, K.S., Pevny, L.H., and Kelley, M.W. (2008). Sox2 signaling in prosensory domain specification and subsequent hair cell differentiation in the developing cochlea. Proc. Natl. Acad. Sci. USA *105*, 18396–18401.

Doetzlhofer, A., Basch, M.L., Ohyama, T., Gessler, M., Groves, A.K., and Segil, N. (2009). Hey2 regulation by FGF provides a Notch-independent mechanism for maintaining pillar cell fate in the organ of Corti. Dev. Cell *16*, 58–69.

Fujioka, M., Okano, H., and Edge, A.S. (2015). Manipulating cell fate in the cochlea: a feasible therapy for hearing loss. Trends Neurosci *38*, 139–144.

Gao, W.-Q. (2003). Hair cell development in higher vertebrates. Curr. Top. Dev. Biol. *57*, 293–319.

Gnedeva, K., and Hudspeth, A. (2015). SoxC transcription factors are essential for the development of the inner ear. Proc. Natl. Acad. Sci. USA *112*, 14066–14071.

Golden, E.J., Benito-Gonzalez, A., and Doetzlhofer, A. (2015). The RNA-binding protein LIN28B regulates developmental timing in the mammalian cochlea. Proc. Natl. Acad. Sci. USA *112*, E3864–E3873.

Huh, S.-H., Jones, J., Warchol, M.E., and Ornitz, D.M. (2012). Differentiation of the lateral compartment of the cochlea requires a temporally restricted FGF20 signal. PLoS Biol. *10*, e1001231.

Kechad, A., Jolicoeur, C., Tufford, A., Mattar, P., Chow, R.W., Harris, W.A., and Cayouette, M. (2012). Numb is required for the production of terminal asymmetric cell divisions in the developing mouse retina. J. Neurosci. *32*, 17197–17210.

Kelley, M.W. (2006). Regulation of cell fate in the sensory epithelia of the inner ear. Nat. Rev. Neurosci. *7*, 837–849.

Kiernan, A.E. (2013). Notch signaling during cell fate determination in the inner ear. Semin. Cell Dev. Biol. *24*, 470–479.

Knoblich, J.A. (2010). Asymmetric cell division: recent developments and their implications for tumour biology. Nat. Rev. Mol. Cell Biol. *11*, 849–860.

Kuo, B.R., Baldwin, E.M., Layman, W.S., Taketo, M.M., and Zuo, J. (2015). In vivo cochlear hair cell generation and survival by coactivation of β-catenin and Atoh1. J. Neurosci. *35*, 10786–10798.

Li, W., Wu, J., Yang, J., Sun, S., Chai, R., Chen, Z.-Y., and Li, H. (2015). Notch inhibition induces mitotically generated hair cells in mammalian cochleae via activating the Wnt pathway. Proc. Natl. Acad. Sci. USA *112*, 166–171.

Liang, J., Wang, D., Renaud, G., Wolfsberg, T.G., Wilson, A.F., and Burgess, S.M. (2012). The stat3/socs3a pathway is a key regulator of hair cell regeneration in zebrafish stat3/socs3a pathway: regulator of hair cell regeneration. J. Neurosci. *32*, 10662–10673.

Mizutari, K., Fujioka, M., Hosoya, M., Bramhall, N., Okano, H.J., Okano, H., and Edge, A.S. (2013). Notch inhibition induces cochlear hair cell regeneration and recovery of hearing after acoustic trauma. Neuron *77*, 58–69.

Munnamalai, V., Hayashi, T., and Bermingham-McDonogh, O. (2012). Notch prosensory effects in the mammalian cochlea are partially mediated by Fgf20. J. Neurosci. *32*, 12876–12884.

Nichane, M., Ren, X., and Bellefroid, E.J. (2010). Self-regulation of Stat3 activity coordinates cell-cycle progression and neural crest specification. EMBO J. *29*, 55–67.

Ono, K., Kita, T., Sato, S., O'Neill, P., Mak, S.-S., Paschaki, M., Ito, M., Gotoh, N., Kawakami, K., and Sasai, Y. (2014). FGFR1-Frs2/3 signalling maintains sensory progenitors during inner ear hair cell formation. PLoS Genet. *10*, e1004118.

Pan, W., Jin, Y., Stanger, B., and Kiernan, A.E. (2010). Notch signaling is required for the generation of hair cells and supporting cells in the mammalian inner ear. Proc. Natl. Acad. Sci. USA *107*, 15798–15803.

Romero-Carvajal, A., Acedo, J.N., Jiang, L., Kozlovskaja-Gumbrienė, A., Alexander, R., Li, H., and Piotrowski, T. (2015). Regeneration of sensory hair cells requires localized interactions between the Notch and Wnt pathways. Dev. Cell *34*, 267–282.

Shi, F., Kempfle, J.S., and Edge, A.S. (2012). Wnt-responsive Lgr5-expressing stem cells are hair cell progenitors in the cochlea. J. Neurosci. *32*, 9639–9648.

Shi, F., Hu, L., Jacques, B.E., Mulvaney, J.F., Dabdoub, A., and Edge, A.S. (2014). β-Catenin is required for hair-cell differentiation in the cochlea. J. Neurosci. *34*, 6470–6479.

Shou, J., Zheng, J.L., and Gao, W.-Q. (2003). Robust generation of new hair cells in the mature mammalian inner ear by adenoviral expression of Hath1. Mol. Cell Neurosci. *23*, 169–179.

Tadokoro, T., Wang, Y., Barak, L.S., Bai, Y., Randell, S.H., and Hogan, B.L. (2014). IL-6/STAT3 promotes regeneration of airway ciliated cells from basal stem cells. Proc. Natl. Acad. Sci. USA *111*, E3641–E3649.

Wang, J., Zhu, H.H., Chu, M., Liu, Y., Zhang, C., Liu, G., Yang, X., Yang, R., and Gao, W.-Q. (2014). Symmetrical and asymmetrical division analysis provides evidence for a hierarchy of prostate epithelial cell lineages. Nat. Commun. *5*, 4758.

White, P.M., Doetzlhofer, A., Lee, Y.S., Groves, A.K., and Segil, N. (2006). Mammalian cochlear supporting cells can divide and trans-differentiate into hair cells. Nature *441*, 984–987.

Woods, C., Montcouquiol, M., and Kelley, M.W. (2004). Math1 regulates development of the sensory epithelium in the mammalian cochlea. Nat. Neurosci. *7*, 1310–1318.

Yang, R., Wang, M., Wang, J., Huang, X., Yang, R., and Gao, W.-Q. (2015). Cell division mode change mediates the regulation of cerebellar granule neurogenesis controlled by the sonic hedgehog signaling. Stem Cell Rep. *5*, 816–828.

Zheng, J.L., and Gao, W.-Q. (2000). Overexpression of Math1 induces robust production of extra hair cells in postnatal rat inner ears. Nat. Neurosci. *3*, 580–586.

Zheng, J.L., Shou, J., Guillemot, F., Kageyama, R., and Gao, W.-Q. (2000). Hes1 is a negative regulator of inner ear hair cell differentiation. Development *127*, 4551–4560.

Zine, A., Aubert, A., Qiu, J., Therianos, S., Guillemot, F., Kageyama, R., and de Ribaupierre, F. (2001). Hes1 and Hes5 activities are required for the normal development of the hair cells in the mammalian inner ear. J. Neurosci. *21*, 4712–4720.